Improving the Performance of Mass-Consistent Numerical Models Using Optimization Techniques

J. C. BARNARD AND H. L. WEGLEY*

Pacific Northwest Laboratory, Richland, WA 99352

T. R. HIESTER**

FloWind Corporation, Pleasanton, CA 94566

(Manuscript received 15 March 1986, in final form 25 November 1986)

ABSTRACT

This paper describes a technique of using a mass-consistent model to derive wind speeds over a microscale region (about 4 km^2) of complex terrain. A serious limitation of these numerical models is that the calculated wind field is highly sensitive to certain input parameters, such as that used to simulate the atmospheric stability. Because accurate values for these parameters are not usually known, confidence in the calculated winds is low.

However, values for these parameters can be found by tuning the model to existing wind observations within a microscale area. This tuning is accomplished with an optimization procedure that adjusts the unknown parameters so that the discrepancy between the observed winds and model calculations of these winds is minimized.

The model was verified with eight sets of hourly averaged wind data. These data were obtained from measurements made at 28 sites covering a windfarm development in the Altamont Pass area of California. When the model was tuned to a small subset of the 28 sites, the model showed skill in predicting wind speeds for the remaining sites in six of the eight cases. The two that did not perform as well were low wind speed cases.

1. Introduction

Wind energy developers are concerned with maximizing the energy capture of a wind turbine development. When such developments are located in areas of complex terrain, large variations in energy production can result from variations in wind that occur over relatively small distances (50–100 m). As a result, developers need tools that identify high wind speeds over areas the size of a wind farm (about 5 km^2). These tools must provide sufficient resolution of the wind flow over the area in three-dimensional space to discriminate clearly between suitable and unsuitable sites. Simulations of wind flow can fill this need for resolution when limited data are available.

Numerical models provide one method of simulating the flow. These models range from the very complex primitive equation models to the relatively simple kinematic models. One type of kinematic model that is designed for use in complex terrain is the mass-consistent model. This model uses observations of the winds made at specific places to calculate a wind field throughout the modeling domain; this allows the estimation of the winds at places away from the observation sites. When compared to the primitive equation models, the relative simplicity of the mass-consistent model makes it attractive for air pollution and wind energy studies, because it does not require much input data and is easy and economical to operate.

These strengths of the mass-consistent model have not led to its wide use for quantitative predictions of windiness in complex terrain. This situation has been caused by two difficulties. The first of these is the sensitivity of the calculated winds to certain model input parameters. Among the most important of these parameters are the stability parameter, used to simulate the effects of atmospheric stability on the calculated wind field, and the initial boundary layer exponent, which controls the vertical extrapolation of the wind during the model initialization. The sensitivity of the calculated winds to these parameters has been investigated through numerical experiments where the parameter in question is varied and the resulting effect on the calculated flow is observed. In this manner, Traci et al. (1979) and Kitada et al. (1983) have demonstrated the large influence on the flow to variations in the model's stability parameter. Additionally, Traci et al. (1979) have shown that the flow is sensitive to the initial boundary layer exponent, as well.

The second difficulty that has beset the mass-consistent model is lack of verification. Wind datasets of sufficient spatial density to provide for both model ini-

* Present Affiliation: Ultrasystems Defense and Space Systems, Inc., Kent, WA 98032.

** Present Affiliation: Flow Industries, Inc., Kent, WA 98032.

tialization and verification have been in short supply; however, a few datasets have been available with which to perform verification experiments. These datasets have been obtained from observation networks over relatively large areas of complex terrain. Verification studies using data taken from the island of Oahu, Hawaii (Traci et al., 1979), and the Nevada Test Site (Traci et al., 1980) have shown that the root-mean-square error between calculated and observed winds is typically 2 to 4 m s^{-1}. Errors of this magnitude are too large to permit the confident use of the mass-consistent model in siting wind turbines over the area of a wind farm; however, the performance of the model may improve substantially when it is applied to such smaller areas, because the spatial density of the wind observations necessary for model initialization is generally greater.

Better estimation of the stability parameter may enhance model performance. For the verification studies cited previously, this parameter was estimated through a crude form of model tuning that entailed operating the model for a number of different stability parameters and then comparing these runs to a single set of averaged wind observations. The stability parameter associated with the model run that best matched the observations was assumed to be the appropriate parameter for all the model runs of the verification exercise. Because this value is not likely to be appropriate for all verification cases, serious degradation in the model's performance may have occurred for some of these cases. If a means had been available for accurately determining the stability parameter for each individual model application, significant improvement might have occurred.

The sensitivity of the flow to the relevant input parameters, normally a major problem, can be turned to the modeler's advantage if wind observations are available for a small number of locations in the area of interest, so that these parameters can be accurately determined for each model run. If this is the case, the model can be precisely tuned by the use of an optimization technique. This technique automatically adjusts the important input variables until they assume "optimum" values; at these values the error between the wind observations and the model-calculated winds is minimized. This paper describes the application of an optimization technique to a mass-consistent model to find optimum values for the important flow variables. The performance of this model is also verified through the use of a wind dataset collected from a spatially dense network of observation sites. The verification shows that, for most cases, reasonably accurate flow simulations can be obtained using a limited amount of wind data.

2. The mass-consistent flow model

Sherman (1978) describes the theory of the mass-consistent model. Observations of the wind are used to construct an initial guess of the wind at every grid point in the modeled area. These initial winds are then adjusted to achieve a final wind field, which departs from the original field only enough to satisfy the equation of mass continuity (hence the name mass-consistent model). The adjustment at grid points adjacent to solid boundaries is done so that the adjusted wind field is parallel to the boundary, the so-called impenetrability constraint. Because these two features of the adjustment are important influences on wind flow in complex terrain, the mass-consistent model is particularly suited for flow simulations in such areas.

The mathematical formulation of the mass-consistent model uses a calculus-of-variations approach originally developed by Sasaki (1958). Let x, y represent the horizontal directions, and z the vertical direction over a modeling domain V. At first, the mass-consistent model constructs an initial guess of the wind components u_0, v_0, w_0 over the entire modeling domain; these components are the wind speeds in the x, y, and z directions, respectively. The initial guesses are formed from an interpolation/extrapolation scheme that uses existing surface wind observations contained within the modeled area. The model then calculates the "adjusted" wind components u, v, w so that the integral

$$I=\int_V \{\alpha_1^2(u-u_0)^2+\alpha_1^2(v-v_0)^2+\alpha_2^2(w-w_0)^2\}dV \tag{1}$$

is minimized, subject to the restriction that the final, adjusted components satisfy the continuity equation

$$\frac{\partial u}{\partial x}+\frac{\partial v}{\partial y}+\frac{\partial w}{\partial z}=0. \tag{2}$$

In (1), α_1 and α_2 are factors weighting the relative amount of adjustment in the horizontal and vertical directions, respectively. These weighting factors play an important role in the operation of a mass-consistent model because they are components of the stability parameter. As previously mentioned, the calculated winds are quite sensitive to the value assigned to this parameter; this sensitivity will be demonstrated in section 3.

The minimization of (1) subject to the constraint (2) is a straightforward problem in the calculus of variations, and is accomplished by introducing a Lagrange multiplier, $\lambda(x, y, z)$. The functional to be minimized is then

$$F=\int_V\left[\alpha_1^2(u-u_0)^2+\alpha_1^2(v-v_0)^2+\alpha_2^2(w-w_0)^2+\lambda\left(\frac{\partial u}{\partial x}+\frac{\partial v}{\partial y}+\frac{\partial w}{\partial z}\right)\right]dV \tag{3}$$

and the associated Euler–Lagrange equations whose solution minimizes (3) are

$$u = u_0 + \frac{1}{2\alpha_1^2}\frac{\partial \lambda}{\partial x}, \tag{4}$$

$$v = v_0 + \frac{1}{2\alpha_1^2}\frac{\partial \lambda}{\partial y}, \tag{5}$$

$$w = w_0 + \frac{1}{2\alpha_2^2}\frac{\partial \lambda}{\partial z}. \tag{6}$$

Substitution of (4)–(6) into (2) yields the governing equation for λ:

$$\frac{\partial^2\lambda}{\partial x^2} + \frac{\partial^2\lambda}{\partial y^2} + \left(\frac{\alpha_1}{\alpha_2}\right)^2 \frac{\partial^2\lambda}{\partial z^2} = -2\alpha_1^2\left(\frac{\partial u_0}{\partial x} + \frac{\partial v_0}{\partial y} + \frac{\partial w_0}{\partial z}\right). \tag{7}$$

This equation is solved for λ; once λ is known throughout the modeling domain, the adjusted velocity components are calculated using (4)–(6).

Sherman (1978) shows that two types of boundary conditions are used when finding the solution to (7). The first of these is that for open or "flow-through" boundaries, $\lambda = 0$. The normal derivative of λ at these boundaries is, in general, not zero, and flow adjustment therefore may occur. Second, at solid surfaces the normal derivative $\partial\lambda/\partial n$ is required to be zero so that no normal adjustment takes place. This boundary condition, along with the requirement that the initial surface flow components be parallel to the surface, satisfies the impenetrability constraint.

An accurate treatment of the lower boundary condition requires that the terrain surface be adequately resolved in both the vertical and the horizontal dimensions. In a Cartesian coordinate system, the terrain is represented in "stair-step" fashion, and the vertical terrain resolution is limited by the vertical distance between grid points. This distance must be much smaller than the terrain relief if adequate vertical resolution is to be achieved. The small vertical zoning required by most model applications can create a very large number of grid points, with a concomitant increase in computational effort. This difficulty can be avoided by casting the model equations into a terrain conformal coordinate system; in this system, the lower boundary becomes a coordinate surface, and a "stair-step" approximation of the surface is no longer necessary. This transformation also has another advantage, variable vertical zoning, which permits a relatively small vertical distance between grid points near the surface while maintaining a coarse resolution aloft. Thus, the winds near the surface, which are of most concern to model users, can be calculated with greater numerical accuracy without resort to fine vertical resolution throughout the modeling domain.

The mass-consistent model used in this paper is the NOABL model described by Traci et al. (1978). This model uses a terrain-conformal coordinate system where a new vertical coordinate, σ, is related to z through the transformation

$$\sigma(x, y, z) = \frac{z_t - z}{z_t - z_s(x, y)} = \frac{z_t - z}{\pi(x, y)} \tag{8}$$

where z_t is the top of the model, assumed to be a constant altitude, and $z_s(x, y)$ is the height of the terrain surface, which is a function of x and y. This coordinate transformation requires that the model equations be recast into forms appropriate to the new coordinate system. As shown by Traci et al. (1978), the equation of continuity (2) in the terrain conformal coordinate system becomes

$$\frac{\partial \pi u}{\partial x} + \frac{\partial \pi v}{\partial y} + \frac{\partial \pi \tilde{w}}{\partial \sigma} = 0 \tag{9}$$

where

$$\pi\tilde{w} = \sigma\left(\frac{\partial z_s}{\partial x}u + \frac{\partial z_s}{\partial y}v\right) - w,$$

the governing Eq. (7) becomes

$$\frac{\partial}{\partial x}\left(\pi\frac{\partial\lambda}{\partial x} + \sigma\frac{\partial z_s}{\partial x}\frac{\partial\lambda}{\partial\sigma}\right) + \frac{\partial}{\partial y}\left(\pi\frac{\partial\lambda}{\partial y} + \sigma\frac{\partial z_s}{\partial y}\frac{\partial\lambda}{\partial\sigma}\right) + \frac{\partial}{\partial\sigma}\left(\left\{\frac{\alpha_1^2}{\alpha_2^2} + \sigma^2\left[\left(\frac{\partial z_s}{\partial x}\right)^2 + \left(\frac{\partial z_s}{\partial y}\right)^2\right]\right\} \times \frac{1}{\pi}\frac{\partial\lambda}{\partial\sigma} + \sigma\left(\frac{\partial z_s}{\partial x}\frac{\partial\lambda}{\partial x} + \frac{\partial z_s}{\partial y}\frac{\partial\lambda}{\partial y}\right)\right) = -2\alpha_1^2\left[\frac{\partial \pi u_0}{\partial x} + \frac{\partial \pi v_0}{\partial y} + \frac{\partial \pi \tilde{w}_0}{\partial \sigma}\right], \tag{10}$$

and the adjusted velocity components are calculated through the following equations:

$$u = u_0 + \frac{1}{2\alpha_1^2}\left(\frac{\partial\lambda}{\partial x} + \frac{\sigma}{\pi}\frac{\partial z_s}{\partial x}\frac{\partial\lambda}{\partial\sigma}\right) \tag{11}$$

$$v = v_0 + \frac{1}{2\alpha_1^2}\left(\frac{\partial\lambda}{\partial y} + \frac{\sigma}{\pi}\frac{\partial z_s}{\partial y}\frac{\partial\lambda}{\partial\sigma}\right) \tag{12}$$

$$w = w_0 - \frac{1}{2\alpha_2^2}\left(\frac{1}{\pi}\frac{\partial\lambda}{\partial\sigma}\right). \tag{13}$$

The governing Eq. (10) is solved numerically for λ by using successive over-relaxation; once λ is known, (11)–(13) yield the adjusted velocities at the model grid points.

As seen through Eqs. (4)–(6) and (11)–(13), the amount of adjustment in the horizontal and vertical directions is proportional to $1/2\alpha_1^2$ and $1/2\alpha_2^2$, respectively. The logarithm of the ratio of these quantities, $\log(\alpha_1/\alpha_2)^2$, forms an important flow parameter that governs the relative adjustment of the vertical to the horizontal direction. This parameter is assigned the symbol τ and it acts as an empirical stability parameter for the model. For τ less than zero, flow adjustment in the horizontal plane predominates, so that an air parcel is more likely to go around a terrain barrier rather than over it, as would occur in a stable atmo-

sphere. In an analogous manner, when τ is greater than zero, the adjustment is primarily in the vertical direction, encouraging flow over an obstacle, thus simulating an unstable atmosphere. The flow adjustment is not given preference in either direction when τ is equal to zero; this represents neutral conditions.

A relationship between the empirical stability parameter, τ, and the actual atmospheric stability as represented by, for example, a Richardson number, has not been discovered. Input values for τ have usually been supplied through educated guesswork or crude forms of model tuning. Because the flow simulations may be quite sensitive to τ, and its appropriate value is usually uncertain, confidence in calculated wind fields in the absence of explicit verification is not justified. The technique to be described in section 3 does not require a priori knowledge of the stability parameter and, in fact, it becomes a quantity that is calculated by the model rather than being an input parameter.

Before beginning the adjustment process to make the wind field mass-consistent, an initial guess of the wind velocity components, u_0, v_0, w_0, must be supplied to all the model grid points. This initial guess is derived from existing wind measurements taken within the modeled area; usually these consist of a small number of surface observations and, therefore, a means must be devised for extrapolating these limited data to all the grid points. There are many possibilities for performing this extrapolation. In the absence of vertical wind speed information, the model considered here uses a simple two-step procedure that first extrapolates each surface observation in the vertical dimension; second, once these vertical soundings are constructed, a horizontal interpolation on each conformal level is used to fill in the grid points with the initial guesses.

The vertical profiles that are made for each observation assume a power law profile below an arbitrarily defined boundary layer height, z_{bl}; above this height the wind speed is constant. If u'_0 is the u-component of the speed for a given surface observation made at a height z_0, the vertical sounding, $u'(z)$, is defined by

$$u'(z) = \begin{cases} \left(\dfrac{z}{z_0}\right)^{\beta} u'_0, & z \leqslant z_{bl} \\ \left(\dfrac{z_{bl}}{z_0}\right)^{\beta} u'_0, & z > z_{bl} \end{cases} \tag{14}$$

where β is the initial boundary layer exponent required as part of the model input. (A similar relationship governs the vertical extrapolation of the v-component.) For all the model calculations presented here, z_{bl} was arbitrarily specified as 200 m. Because wind shear information was not available, β was arbitrarily taken to be 0.14 (i.e., conformance with the $\frac{1}{7}$ power law).

Once the vertical soundings are constructed, horizontal interpolation on a conformal surface is performed to fill in the grid points with u_0 and v_0. The contribution from each sounding to the initial velocity components at the grid point in question is weighed by $1/r^2$, where r is the horizontal distance from the grid point to the sounding. This is the well-known $1/r^2$ interpolation technique. If only one station is used for model initialization, then only one sounding is produced, and the horizontal interpolation is not necessary. In this case, the initial guesses of the wind (u_0, v_0) on a given conformal surface are constant over the surface, and they are the components of the sounding evaluated at the height of the conformal surface over the observation site. The initial vertical velocity, w_0, is set equal to zero at all grid points, except at the lower boundary. There w_0 is calculated so that the initial wind is parallel to the terrain surface.

3. Applying optimization techniques to a mass-consistent model

An optimization technique is merged with a mass-consistent model to automatically and accurately provide model tuning. This combination will hereafter be referred to as the "model." The model requires as input wind observations taken at a number of sites over the area of interest. These sites are called tuning sites and they serve two purposes. First, at least one of the tuning sites is required for the model initialization, as described in section 2. For this paper, a very simple initialization was performed where only one site (the reference site) was used to initialize the model. This initialization could be easily modified if desired.

The second purpose of the tuning sites is, as the name implies, for model tuning. The error between the calculated winds and the observed winds at the tuning sites forms a basis for gauging the model's performance. During the tuning process, the optimization procedure adjusts τ (and the initial wind direction) until this error is minimized. The results shown later in section 4 confirm that when this error is small, the accuracy of model-estimated winds away from the tuning sites is high.

To cast the optimization procedure into mathematical terms, assume that there are N wind observation sites distributed over a microscale region. (For the verification studies described later, N ranged from 6 to 8.) The station with the highest average wind speed is designated the reference site and is used to initialize the model. For a given averaging period, the wind speeds are normalized by the reference site wind speed. This gives a set of ratios, r_i^o, for each set of averaged wind data, where the subscript i denotes the station i and o denotes that these are observed ratios. The reference site ($i = 1$) speed is normalized by itself so that $r_i^o = 1$. A corresponding set of calculated ratios can be derived by operating the model with a given set of input data and then normalizing the speeds calculated for the tuning sites by the speed calculated at the reference site. These ratios are denoted by r_i^c, where c denotes calculated ratio; they are considered a function of only

the atmospheric stability, τ, and the initial wind direction, θ.

The initial wind direction is the direction used to construct the initial guess of the wind field before the adjustment to conserve mass is made [i.e., if s is the reference site wind speed, u'_0 in (14) is given by $-s(\sin\theta)$; v'_0 is $-s(\cos\theta)$]. This direction can be thought of as an estimate of the direction of the mean flow for the particular case under consideration. For the data used in this study, a measurement of the wind direction was made only at the reference site. Because this measurement could be influenced by the local terrain, it may not represent the actual direction of the mean flow. Because of this difficulty, and the sensitivity of calculated ratios to variations in the initial wind direction, the initial direction is included as a parameter of the optimization procedure. To explicitly show the dependence of r_i^c on both τ and θ, it will be written as $r_i^c(\tau, \theta)$.

A measure of the goodness of fit between the calculated and observed ratios is the root-mean-square error, RMSE, given by the expression

$$\mathrm{RMSE}(\tau,\theta) = \{\sum_{i=1}^{N} [r_i^o - r_i^c(\tau,\theta)]^2/N\}^{1/2}. \quad (15)$$

Since the calculated ratios, $r_i^c(\tau, \theta)$, depend upon τ and θ, the error is also a function of these quantities, as is indicated above.

The root-mean-square error can be depicted as a three-dimensional surface; the height of the surface is a function of τ and θ. Figure 1 shows the surface for one of the wind datasets used in this study (case 3B; these data are described in the next section). The abcissae for this figure are the wind direction, θ, and the stability parameter, τ, which ranges from -2 (stable) through 0 (neutral) to $+2$ (unstable). Figure 1 shows that, for this particular dataset, the root-mean-square error is much more sensitive to changes in τ than to changes in θ. To better illustrate the sensitivity of RMSE(τ, θ) to stability, Fig. 2 shows RMSE(τ, θ) as a function of τ for a fixed value of θ, 238°. This graph shows that the model-calculated winds are quite sensitive to τ and that departures of τ from its optimum value can cause large increases in the RMSE. However, in previous applications of mass-consistent models there has usually been an absence of guidance on choosing an appropriate value for τ. If for this case one had guessed that $\tau = -2$, the value customarily used for flows assumed to be somewhat stable, the RMSE would have increased fivefold over its minimum value.

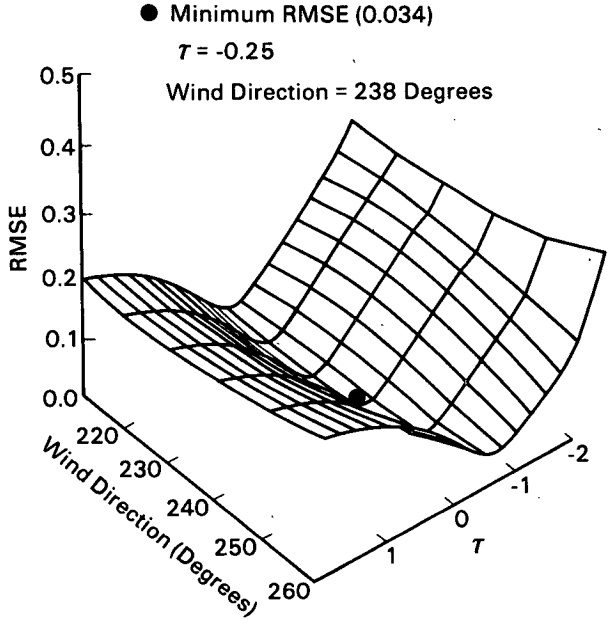

FIG. 1. Sensitivity of the RMSE to the wind direction and stability parameter τ. The minimum RMSE is indicated by the black dot. At this point $\tau = -0.25$, $\theta = 238°$ and RMSE = 0.034.

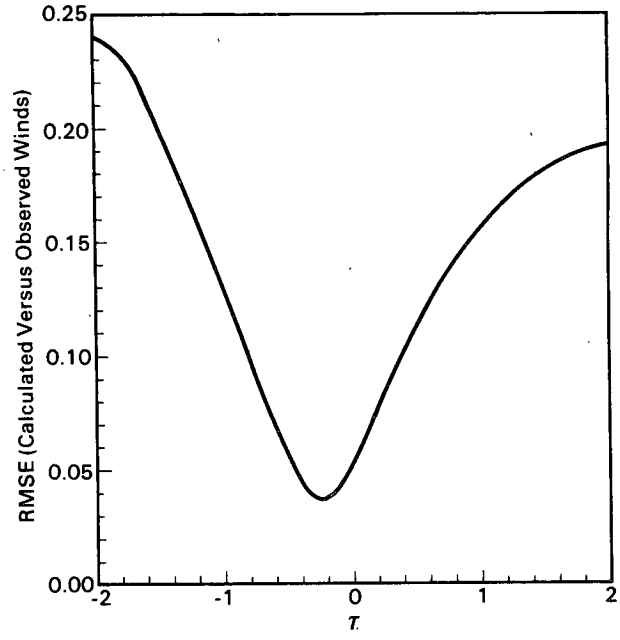

FIG. 2. Sensitivity of the RMSE to the stability parameter τ. The wind direction is assumed to be fixed at its optimum value, 238°.

The "best fit" of the calculated to the observed ratios is obtained when RMSE(τ, θ) is a minimum. The error is minimized in practice by using a nested set of identical minimization algorithms, one for each variable. Starting from initial guesses of θ and τ, the algorithms act alternately on these variables until the minimum RMSE is found. For the RMSE depicted in Fig. 1, the minimum error occurs when $\tau = -0.25$ and $\theta = 238°$. This minimum point is indicated by the black dot on the surface. About one-half hour of VAX 11/780 CPU time was required for the minimization procedure; this time is typical for the other cases considered in this paper, as well.

The algorithm applied to each variable is a single-variable, unconstrained optimization scheme similar to the Coggins algorithm (Kuester and Mize, 1973). This scheme does not rely upon the evaluation of derivatives. It is desirable to avoid the use of derivative-based minimization schemes such as steepest descent, because of the exceptionally large computational effort required to numerically calculate derivatives that are sufficiently accurate to be useful to these schemes.

It is not necessary to restrict the parameters that are optimized to just τ and θ. Other parameters could also be included. The important point is to include those parameters for which the RMSE shows the greatest sensitivity; initial testing has indicated that it is most sensitive to τ and, to a lesser extent, θ. A third parameter that was subject to sensitivity testing was the initial boundary layer exponent, β. The first step of this testing was to operate the model for a fixed value of β equal to 0.14. After the optimization was complete, the optimum values of τ and θ were noted, along with calculated ratios, $r_i^c(\tau, \theta)$, at the tuning sites. Next, β was set to a different value and the model was again operated. For all values of β considered (0.07, 0.11, 0.18, 0.21), the calculated ratios and the optimum value for θ remained essentially unchanged. Significantly, however, the optimum value for τ did change for each value of β different from 0.14. To a good degree of approximation, the relationship between changes in the optimum value of τ and changes in β is $d\tau/d\beta \sim 2.5$. Thus, when β is altered from 0.14 to 0.07, τ is reduced by 0.175. Although this is not a large change for τ, which varied from about -1.5 to 0 between the model runs considered here, it does illustrate that the optimum τ may be influenced by values specified for at least one of the model input parameters.

In summary, this technique minimizes the discrepancy between wind observations and model calculations of the wind at the tuning sites. This minimization is a function of two variables, τ and θ. If the minimum error is sufficiently small, estimates of the wind ratios away from the observation sites are good, and a priori knowledge of the stability parameter is not necessary.

4. Model verification

Data were obtained from a 2 km × 2 km wind farm development near Altamont Pass, California. Figure 3 presents the terrain configuration of the modeled area and the location of the data sites used. The contours shown are drawn from a grid of terrain heights taken at 50-m horizontal intervals. Because the flow model's run time increases dramatically as the grid resolution increases, the 50-m grid interval was selected to minimize the number of grid points and yet to provide enough resolution to represent the features that might affect wind flow over the area.

Data available for the testing of the flow model were hourly averaged wind speed and direction at one reference site, and simultaneous hourly averaged wind speeds for up to 27 other sites. These data were collected for eight cases, described in Table 1. All observations were at a height of 14.03 m above ground. Wind speeds varied from light to moderate (4.5 to 8.5 m s^{-1} in case 2B), to very strong (9.8 to 19.7 m s^{-1} in case 3A). The wind direction was known for only the reference site. Wind directions are all from the southwest quadrant (225° to 250°), the prevailing wind direction for the area.

Atmospheric stability (estimated from wind speed and time of day) appears to vary somewhat over the eight cases. Cases 4B and 5B represent moderate and strong nighttime winds, respectively; cases 2A and 3A represent moderate and strong afternoon winds, respectively; and cases 4A and 5A represent moderate and strong evening winds, respectively. Thus, the dataset to some degree tests the selection of appropriate stability parameters by the optimization scheme.

To test the hypothesis that optimal flow model parameters can be determined with limited observations, the 28 sites where data were collected were separated into a set of eight tuning sites (shown in Fig. 3 as circles), and a set of 20 verification sites (shown as squares). The number and locations of the tuning sites were chosen to reflect the scope of a typical wind measurement program for assessing the wind resource over a microscale region. Table 2 summarizes the data used for model testing and verification. To identify the stations listed in this table with their locations, the site reference numbers (column 1 of Table 2) are plotted within the squares and circles of Fig. 3.

One tuning site was selected as the reference site. This site is indicated by the circle with the superscript R in Fig. 3. Model parameters were adjusted for each of the eight cases by the optimization procedure described in section 3, using the data from the tuning sites. In two cases, data were available from only six of the tuning sites; in three other cases, data from only seven tuning sites were available. This variation in the number of sites that could be used for optimizing (from 6 to 8) had no noticeable effect upon the model's performance. The number of tuning sites used for each case is shown in Table 3.

TABLE 1. Wind data used for testing model: case descriptions.

Case	Date (1984)	Time (LST)	Wind at reference site: Speed (m s^{-1})	Wind at reference site: Direction (°)
2A	30 Oct	1500–1600	9.8	250
2B	13 Nov	1100–1200	8.5	240
3A	26 Oct	1400–1500	19.7	225
3B	2 Nov	1500–1600	18.3	240
4A	27 Oct	1900–2000	8.5	240
4B	1 Nov	2300–2400	9.8	250
5A	26 Oct	1900–2000	17.0	230
5B	13 Nov	0200–0300	18.3	235

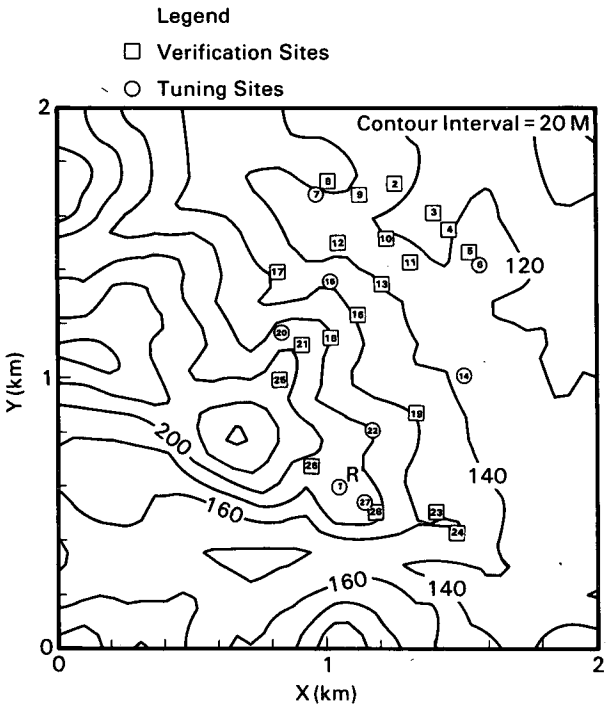

FIG. 3. Terrain contours for the modeled area. The contours are at 20 m intervals. The location of the wind observations used for this study are indicated by the squares and circles: the squares are the verification sites and the circles are the tuning sites. The circle with the superscript R is the reference site. The numbers within the squares and circles correspond to the site reference number in column 1 of Table 2.

The results of the model tuning procedure for the eight wind cases examined are presented in Table 3. Root-mean-square errors (RMSEs) were used as measures of the goodness of fit of the modeled to observed wind speed ratios. Two of the cases shown in Table 3, cases 4A and 4B, exhibit a poor fit between observed and calculated data. Implications of this lack of fit, or poor tuning of the model, are discussed later in this section.

Table 3 also contains the RMSE for each of the eight sets of verification data. Comparison of these data with the tuning site data in this table reveals that there is a slight deterioration in accuracy for the six well-tuned cases as indicated by the RMSE; however, there is a much larger deterioration for the two poorly tuned cases (4A and 4B). A comparison of the average ratios of six cases (i.e., the eight cases excluding 4A and 4B) shows that the overall RMSE becomes 0.037 for the verification site ratios. This value is smaller than that for any individual case, which is expected since random errors between model-calculated winds and wind observations tend to cancel when averages are taken. Figure 4, a scatter plot of observed versus modeled ratios for the six well-tuned cases, clearly demonstrates the skill of the flow model when proper values of the input parameters are selected.

It is interesting to compare the verification RMSE calculated from averaged ratios of the six well-tuned cases to the verification RMSEs obtained from the same cases without model tuning. If θ is taken to be the reference site direction for the case in question, the averaged RMSEs equal 0.059, 0.203, 0.330 when τ equals 0, -1, -2, respectively. As mentioned above, the RMSE obtained from the tuned model runs was 0.037. This comparison shows the benefit of model tuning, which yields explicit, optimum values for τ and θ. Without this guidance, one might operate the model setting τ at -2, resulting in a ninefold increase in the RMSE over that obtained with tuning. A fortuitous guess of $\tau = 0$ would have led to a RMSE not drastically different from the RMSE obtained from tuning. However, without model tuning, there would have been little basis to choose this value of τ over any other.

It is important to note that, for the eight cases under consideration, a correlation exists between the tuning and verification RMSEs, as shown in Fig. 5, where verification RMSEs are plotted against tuning RMSEs. This correlation suggests that the quality of model results can be identified from the magnitude of the tuning RMSE. The eight cases considered in this paper are too few to firmly establish a relationship between the tuning and verification RMSEs. However, this relationship can be estimated by fitting a line of regression to these data; this is shown by the solid line in Fig. 5. If well-tuned model results are arbitrarily defined as those results with a verification RMSE less than about 0.1, the line of regression indicates that the tuning RMSE associated with this definition is about 0.065. Thus, all model results are defined as being well-tuned, with the exception of cases 4A and 4B, which have tuning RMSEs much greater than 0.065. To further illustrate the differences between good model performance and poor performance, scatter plots of wind-speed ratios are presented in Fig. 6 for all the cases.

It is noteworthy that the flow model was poorly tuned only when the winds were light to moderate (i.e., 4.5 to 8.9 m s^{-1}) over the area of interest. These poor results could be caused by applying the model, which can only simulate steady state flow, to situations when the actual flow was far from steady during the averaging period of the observations. For modeling purposes, steady state flow occurs when the influence of the terrain on the flow does not vary over the averaging period. When significant direction fluctuations occur, the terrain's influence is no longer constant because the wind strikes the terrain features at different angles. Direction fluctuations tend to occur more frequently for lower speeds; at higher speeds the direction is usually relatively constant. Therefore, the model's reliability may suffer when applied to low-speed flows during which the direction was not constant. This may explain in part the poor results for two of the four low-speed cases.

Even when the model was well tuned and performed well, the model tended to overpredict the ratios at lower

TABLE 2. Wind data used for testing model: observations by site.

Site ref. no.	Wind speeds (m s^{-1}) by case							
	2A	2B	3A	3B	4A	4B	5A	5B
1[a]	9.8	8.5	19.7	18.3	8.5	9.8	17.0	18.3
2	8.0	5.4	13.0	11.2	8.0	6.7	12.5	8.9
3	7.2	4.5	10.7	10.3	6.3	8.9	11.2	9.4
4	7.6	4.9	12.1	10.7	6.7	8.9	12.1	9.4
5	7.6	5.4	9.8	13.9	8.5	7.6	13.9	10.3
6[a]	8.5	5.8	13.4	12.1	7.6	9.4	12.5	10.7
7[a]	8.5	5.8	13.9	12.5	9.4	8.9	13.4	10.7
8	9.4	6.3	15.6	13.9	9.8	8.9	14.8	12.1
9	8.9	—	14.3	13.0	8.5	8.9	13.9	—
10	7.6	4.5	10.7	9.8	6.3	8.0	10.3	8.0
11	7.6	4.9	11.2	10.3	6.3	8.9	11.2	9.4
12	7.6	4.5	11.6	9.8	6.7	7.6	11.2	7.2
13	6.7	4.9	11.2	10.3	5.4	8.5	11.2	9.4
14[a]	7.6	—	13.0	11.6	5.4	7.6	11.2	—
15[a]	8.0	5.4	12.1	11.6	7.2	8.5	11.6	8.9
16	7.2	5.4	11.2	10.7	6.7	7.6	11.6	10.3
17	7.6	5.4	12.1	10.7	6.7	7.6	12.1	9.4
18	7.6	6.3	13.0	12.5	7.2	7.6	12.5	12.1
19	7.2	6.3	13.4	12.5	4.9	7.6	11.6	12.1
20[a]	8.0	6.3	—	13.4	—	7.6	—	12.5
21	8.0	5.8	—	13.9	—	7.2	—	12.1
22[a]	7.6	—	15.2	13.4	4.9	7.2	12.5	—
23	8.9	7.2	—	14.8	—	8.9	14.3	14.3
24	8.0	7.2	15.6	13.4	7.2	8.0	13.4	12.5
25	6.7	5.8	15.2	14.3	7.2	7.2	13.4	12.5
26	8.5	7.6	17.9	15.6	6.7	8.0	14.3	17.0
27[a]	9.4	8.5	19.7	17.4	8.5	8.9	16.1	16.1
28	9.4	7.6	18.8	15.6	8.0	8.0	14.8	15.2

[a] Tuning sites—site 1 is the reference site.

wind speeds. For example, in case 3A calculated ratios between 0.5 and 0.7 were about 10% higher than the observed ratios. The magnitude of this overprediction may not be solely due to the simplified physics of the model. The effect could also be due to the nature of the objective function (the root-mean-square error) that is minimized during the tuning process. The absolute error at a site is merely the difference between calculated and observed wind-speed ratios. The objective function is comprised of a sum of the squared absolute errors. This formulation for the objective function tends to produce a constant absolute error from site to site at the end of the tuning procedure. Consequently, the relative error, which is the absolute error divided by the observed wind-speed ratio, is usually larger for the lower wind speeds simply because of the division by a smaller number.

Table 4 shows the optimum values of τ and θ derived by the model. The model-derived wind direction is the direction that, when used to make the initial guess of

TABLE 3. The rms error for tuning and verification sites. Note that N is the number of tuning sites.

Case	Reference site: Direction (°)	Reference site: Speed (m s^{-1})	N	Tuning RMSE of ratios	Verification RMSE of ratios
2A	250	9.8	8	0.042	0.080
2B	240	8.5	6	0.042	0.060
3A	225	19.7	7	0.045	0.074
3B	240	18.3	8	0.034	0.050
4A	240	8.5	7	0.126	0.175
4B	250	9.8	8	0.075	0.154
5A	230	17.0	7	0.048	0.047
5B	235	18.3	6	0.056	0.067
All 8 cases:				0.050	0.052
6 cases (excluding 4A and 4B):				0.039	0.037

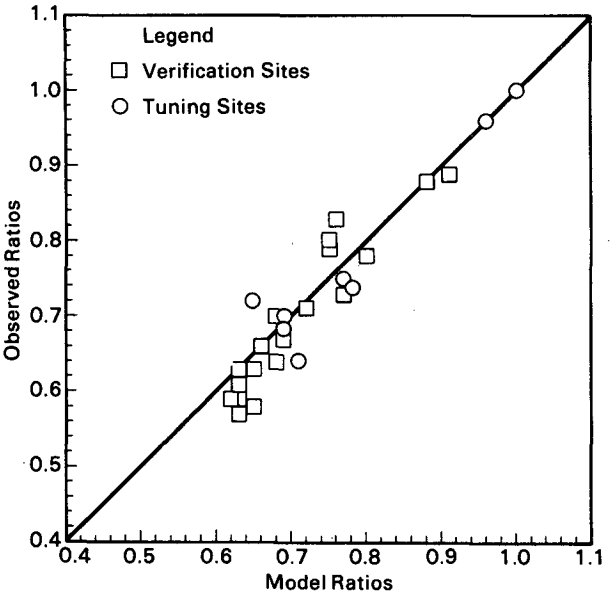

FIG. 4. Scatter plot of observed wind speed ratios vs model-calculated wind speed ratios. These ratios are averages of the six well-tuned cases.

the wind field, yields the lowest tuning RMSE. As mentioned previously, this direction represents an estimate of the direction of the mean flow and may vary significantly from the reference site direction, which is a measurement at a single point in the modeling domain. Despite this limitation, the derived directions roughly agree with the reference site directions. The difference between the two directions exceeds 30° only for cases 4A and 4B, when the model was poorly tuned.

Measurements of vertical gradients of temperature and wind speed are not available for the modeled area. Thus, it is not possible to calculate an accepted measure of the stability, such as the Richardson number, to compare to the model-derived stabilities. This comparison awaits the availability of wind dataset that includes measurements of both the wind and the atmospheric stability. When performing this comparison, it will be important to be aware of the sensitivity of the optimum value of τ to factors other than the actual stability. For example, as has been previously mentioned in section 3, τ is a function of the initial boundary layer profile, β. Often, appropriate values for β are not known because of a lack of wind shear information; because β can be expected to vary between model runs, the discovery of a relationship between the optimum τ and the actual stability is made more difficult. The optimum value for τ may also be influenced by the method of model initialization, other model input parameters, and even the terrain to which the model is applied. The possible strong sensitivity of τ to these factors may further obscure the relationship between τ and the actual stability.

Model-derived horizontal wind speeds for a typical well-tuned case (3A) are shown in Fig. 7. In this figure, the wind speeds are depicted by wind speed contours at 2 m s^{-1} intervals. (These contours are the thick black lines.) The speeds were calculated for a height of 14 m above the ground level (AGL), the same height as that of wind observations. The dashed lines in this figure are the terrain contours shown in Fig. 3.

To facilitate the comparison between the calculated wind field and the wind observations, the wind observations for case 3A are represented in Fig. 7 by numbers that are the wind speed rounded to the nearest meter per second. The numbers are located at both the tuning sites, where they are underlined, and at the verification sites. (These numbers can be distinguished from the wind speed contour labels by their smaller physical size.)

The observations for the southwest winds of case 3A reveal these gross characteristics of the flow: it is accelerated to a speed of about 20 m s^{-1} as it passes over the higher terrain features in the modeling domain, and after passing over these features, the speeds smoothly decrease to about 11–12 m s^{-1} in the northeast corner of the modeled area. The calculated flow agrees quantitatively quite well with the observations, except that the calculated speed is somewhat greater than the observed speed in the relatively flat terrain in the northeast section of the modeling domain. Here

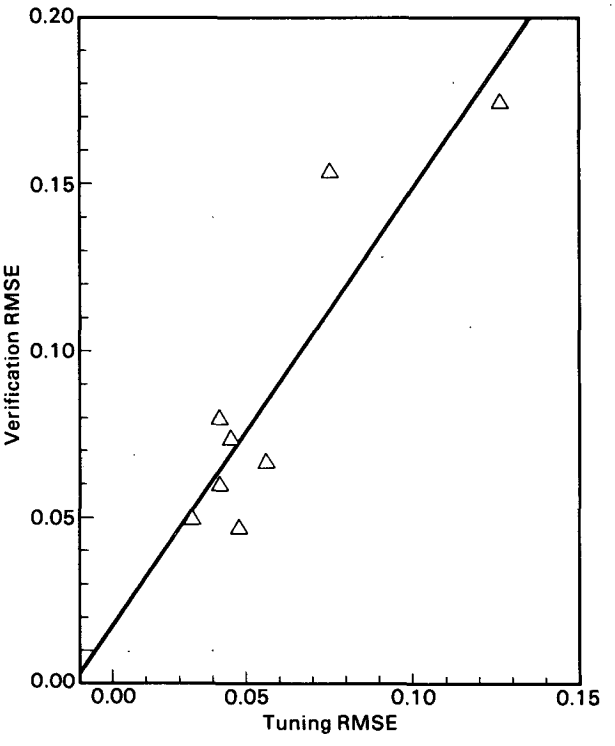

FIG. 5. Scatter plot of the verification RMSE versus the tuning RMSE. The solid black line is a line of regression fit to these points.

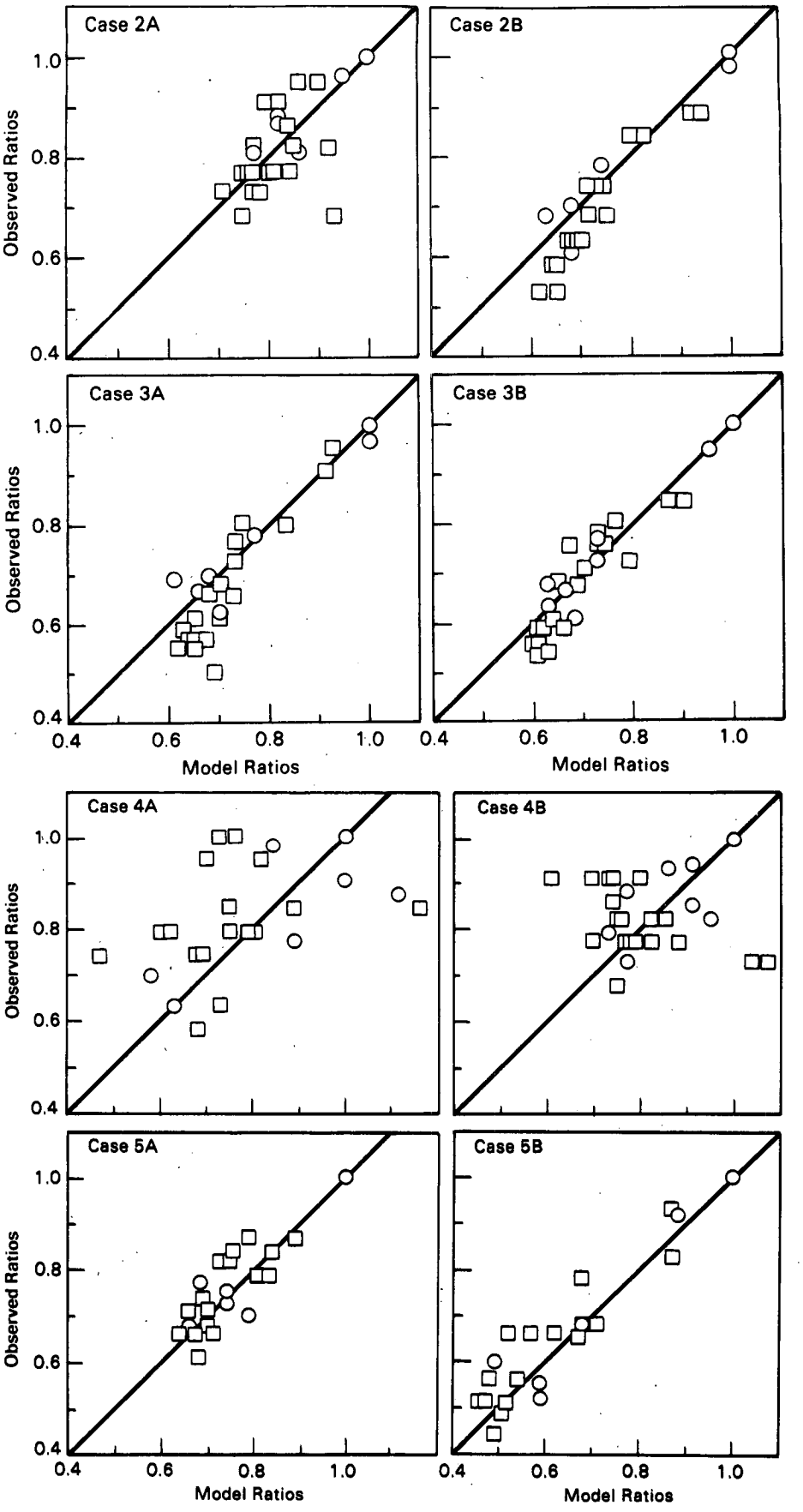

FIG. 6. Scatter plots of observed wind speed ratios versus model-calculated wind speed ratios for all eight cases. The circles are the tuning site ratios, the squares are the verification site ratios.

TABLE 4. Model-derived stability parameters and wind directions for the eight cases.

Case	Direction (°)	τ
2A	266	0.06
2B	222	−0.08
3A	225	−0.05
3B	238	−0.25
4A	282	−1.65
4B	280	−0.71
5A	253	−0.14
5B	245	−0.98

the calculated speeds are in a range of 12–14 m s^{-1}, yet many of the observations are less than 12 m s^{-1}. This again illustrates the model's tendency to overpredict the lower wind speeds.

Vertical velocities calculated for case 3A are shown in Fig. 8 as wind speed contours at 2 m s^{-1} intervals. Like the horizontal speeds, the vertical velocity contours were calculated for a height of 14 m AGL. Vertical velocities were not measured, so observed and calculated velocities cannot be compared. However, the calculated velocities do appear to be realistic. A maximum of about 4 m s^{-1} occurs just upwind of the highest terrain feature in the modeled area. In this area the terrain slope is about 40%, and the horizontal wind speed is about 16 m s^{-1}. Neglecting all physical influences on the flow other than nondivergence, and assuming that the flow at 14 m AGL is parallel to the terrain slope, the vertical velocity could be crudely estimated by the expression

$$w \sim \text{slope} \times \text{horizontal speed}. \quad (16)$$

Thus, for this area , $w \sim 0.4 \times 16$ m s^{-1}, or $w \sim 6$ m s^{-1}. The model-calculated velocity is less than this estimate, which is not surprising since the flow tends to "flatten out" as the height above the terrain surface increases. Hence, the effective slope of the flow at 14 m AGL is less than the assumed 40%, and the vertical velocity just estimated would be too large.

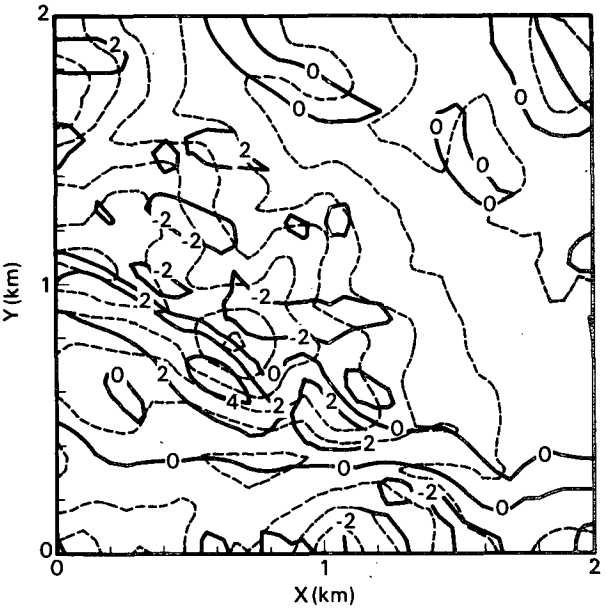

FIG. 8. Contours at 2 m s^{-1} intervals of model-calculated vertical velocities.

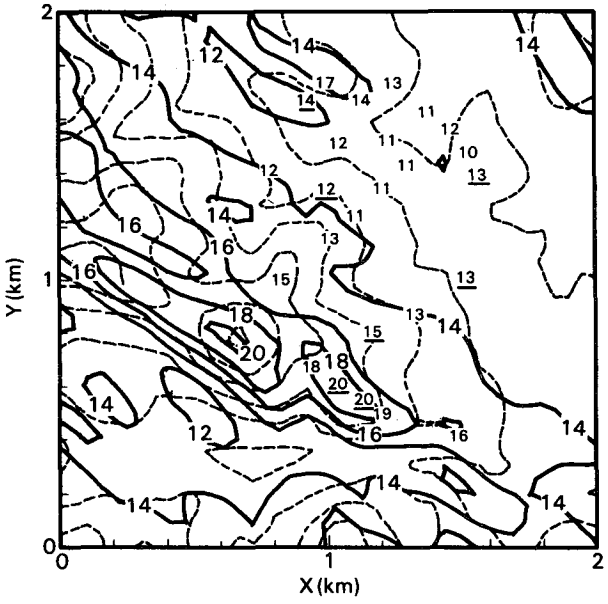

FIG. 7. Contours at 2 m s^{-1} intervals of model-calculated horizontal wind speeds for case 3A. The contours are the thick black lines and they are superimposed over dashed terrain contours. The wind observations for this case are indicated by smaller-sized numbers that are the observed speeds rounded to the nearest meter per second. The tuning sites are underlined.

5. Conclusions

The work presented here has shown that a major obstacle in the use of mass-consistent models—the uncertainty associated with important model input parameters—can be overcome by tuning the model to wind observations within the modeled area. In this paper, the parameters for which values were sought were the stability parameter, τ, and the initial wind direction, θ. Tuning to a specific set of observations results in optimum values for these two parameters for the period over which the wind observations were averaged.

Eight sets of hourly averaged wind data were available for model tuning and testing. When optimum parameters were used to calculate the winds over the modeled area, the model produced good results for six of the eight datasets. In these cases, the RMSE between observed and calculated wind speed ratios was less than

0.08. The two cases that did not perform as well involved low wind speeds. The correlation between tuning RMSE and verification RMSE suggests that the magnitude of the tuning RMSE can warn the model user that the results of a particular run could be seriously in error.

Examination of the optimum wind directions shows that these directions are physically reasonable, as they are in rough agreement with the only measurement of wind direction made in the modeled area. As measurements of the atmospheric stability were not made at or near the modeled area, it was not possible to compare model-derived stability parameters (τ) to actual stabilities. Because τ may be sensitive to factors other than the actual stability, the discovery of a relationship between these two quantities may be difficult.

Acknowledgments. This work was supported by the U.S. Department of Energy under Contract DE-AC06-76RL0 1830. The authors thank Dr. L. L. Wendell for his constant encouragement and his interest in this project. We also thank Drs. C. Doran and T. Horst, Ms. Elizabeth Owczarski, and Laurel Grove for their many helpful suggestions concerning this manuscript.

REFERENCES

Kitada, T., A. Kaki, H. Ueda and L. K. Peters, 1983: Estimation of vertical air motion from limited horizontal wind data—a numerical experiment. *Atmos. Environ.*, **17**, 2181–2192.

Kuester, J. L., and J. H. Mize, 1973: *Optimization Techniques with Fortran.* McGraw-Hill, 500 pp.

Sasaki, Y., 1958: An objective analysis based on the variational method. *J. Meteor. Soc. Japan,* **36,** 77–88.

Sherman, C. A., 1978: A mass-consistent model for wind fields over complex terrain. *J. Appl. Meteor.*, **17**, 312–319.

Traci, R. M., G. T. Phillips and P. C. Patnaik, 1978: *Developing a Site Selection Methodology for Wind Energy Conversion Systems.* DOE/ET/20280-3, [N.T.I.S., Springfield, Virginia], 296 pp.

——, —— and K. C. Rock, 1979: *Wind Energy Siting Methodology Windfield Model Verification Program. I. Oahu, Hawaii, Data Set.* DOE/ET/20280-79/3, [N.T.I.S., Springfield, Virginia], 176 pp.

——, D. C. Wyatt, P. C. Patnaik and G. T. Phillips, 1980: *Wind Energy Siting Methodology Windfield Model Verification Program. II. Nevada Test Site Data Set.* DOE/ET/20280-80/2, [N.T.I.S., Springfield, Virginia], 138 pp.